30 Oct 89 Interim

A Homing Missile Guidance Law Based on New Target Maneuver Models

C: F08635-87-K-0417

Jason L. Speyer; Minjea Tahk; Kevin D. Kim

Debra Harto, AFATL/FXG Program Manager

University of Texas at Austin
Department of Aerospace Engineering
and Engineering Mechanics
Austin, Texas 78712-1085

AFATL-TP-90-01

Air Force Armament Laboratory
AFATL/FXG
Eglin Air Force Base, Florida 32542-5434

Technical Paper

By using more realistic a priori knowledge about the target motion, tracking of maneuvering targets for homing missiles is enhanced. Since certain targets are assumed to execute evasive maneuvers orthogonal to their velocity vector, a new stochastic dynamic target model is proposed where this orthogonality is embedded. Along with this new acceleration dynamic model, the orthogonality is also enforced by the addition of a fictitious auxiliary measurement. The target states are estimated by the modified gain extended Kalman filter (MGEKF), and the angular target maneuver rate is constructed on-line. A guidance law that minimizes a quadratic performance index subject to the assumed stochastic engagement dynamics that includes state dependent noise is derived. This guidance law is determined in closed form where the gains are an explicit function of the estimated target maneuver rate as well as time to go. The numerical simulation for the two-dimensional angle-only measurement case indicates that the proposed target model with the MGEKF leads to remarkable estimation of the target states. Furthermore, the effect on terminal miss distance using this new guidance scheme is given.

Kalman filter, target estimation, linear quadratic guidance law, guidance law

34

UNCLASSIFIED UNCLASSIFIED UNCLASSIFIED SAR

A Homing Missile Guidance Law Based on New Target Maneuver Models

Jason L. Speyer [1], Kevin D. Kim[2], and Minjea Tahk[3]

Dept. of Aerospace Engineering and Engineering Mechanics
University of Texas at Austin, Austin, TX, 78712

Abstract

By using more realistic a priori knowledge about the target motion, tracking of maneuvering targets for homing missiles is enhanced. Since certain targets are assumed to execute evasive maneuvers orthogonal to their velocity vector, a new stochastic dynamic target model is proposed where this orthogonality is embedded. Along with this new acceleration dynamic model, the orthogonality is also enforced by the addition of a fictitious auxiliary measurement. The target states are estimated by the modified gain extended Kalman filter(MGEKF), and the angular target maneuver rate is constructed on-line. A guidance law that minimizes a quadratic performance index subject to the assumed stochastic engagement dynamics that includes state dependent noise is derived. This guidance law is determined in closed form where the gains are an explicit function of the estimated target maneuver rate as well as time to go. The numerical simulation for the two-dimensional angle-only measurement case indicates that the proposed target model with the MGEKF leads to remarkable estimation of the target states. Furthermore, the effect on terminal miss distance using this new guidance scheme is given.

---

[1]Harry H. Power Professor in Engineering, Fellow, AIAA
[2]Graduate Research Assistant, Student Member AIAA
[3]Research Engineer, Integrated Systems, Inc., Santa Clara, CA, 95054, Member AIAA

1. Introduction

The target tracking problem for homing missile guidance involves the estimation of problems of estimating large and rapidly changing target accelerations. The time history of target motion is inherently a jump process where the acceleration levels and switching times are unknown a priori. Due to this arbitrary and unpredictable nature of target maneuverability, target acceleration cannot easily be modeled.

A considerable number of tracking methods for maneuvering targets have been proposed and developed for both new target models and filtering techniques[1]-[7]. In spite of the numerous modeling and filtering techniques available, target acceleration estimation using angle-only measurements is relatively poor. Usually, the target tracking problem is approached by modeling target acceleration with a first-order Gauss-Markov model and applying the extended Kalman filter(EKF). One difficulty with the Gauss-Markov model is that the assumed large process noise spectral density induces Kalman filter divergence even when the target maneuver is not present and can lead to a target acceleration magnitude estimate which exceeds the actual maximum. Another problem is that the target motion is not well represented by Gauss-Markov diffusion process.

In an effort to alleviate these problems, the circular target model has been proposed as a target motion model, where the phase angle is a Brownian motion process and the acceleration magnitude can be either a random variable or a bounded stochastic process. This target model was suggested in [4] using concepts extracted from [9,10].

By including a priori knowledge of the target motion, improved estimates of the target states can be obtained. This idea is included in [6,7] by using a target acceleration model which employs a target mean jerk term. For conventional targets such as winged aircraft, the longitudinal acceleration component is often negligible compared to the lateral component in evasive maneuvers. This notion fits the circular target model where the angular rate term is estimated to account for the actual dynamics of the coordinated turn. This model is presented in Section 2. However, an approximate

state expansion is required to handle the unknown angular rate in the target model. This approximate dynamical system used for estimation is presented in Sections 3.1 and 3.2. Furthermore, in Section 3.3 the orthogonality between target velocity and acceleration can be viewed as a kinematic constraint where compliance is inforced by including this constraint as a pseudo-measurement[7,8]. The approximate target dynamics and pseudomeasurement are included in the modified gain extended Kalman filter(MGEKF)[11] and is presented in Section 4. The MGEKF is selected because of its superior performance over the EKF especially for bearing-only problems. In Section 5, a linear quadratic guidance law is derived for this circular target model. This guidance law remains a linear function of the estimated states, but the guidance gains obtained in closed form are a nonlinear function of the estimated rotation rate and time to go. Finally, a numerical simulation is performed for a two-dimensional homing missile intercept problem. Both the estimation process and the terminal miss are enhanced by the new models and the associated estimator and guidance law.

2. Target Acceleration Model

In this section the circular target acceleration model is presented, and the dynamic consistency between this target model and an assumed nonlinear target model is discussed.

2.1. Circular Target Motion

The two-dimensional homing missile guidance scenario is described by two sets of nonlinear dynamic equations of motion for the missile and target

$$\begin{array}{rclcrcl} \dot{x}_M &=& V_M cos\theta_M & , & \dot{x}_T &=& V_T cos\theta_T \\ \dot{y}_M &=& V_M sin\theta_M & , & \dot{y}_T &=& V_T sin\theta_T \\ \dot{V}_M &=& a_{M_t} & , & \dot{V}_T &=& 0 \\ \dot{\theta}_M &=& a_{M_n}/V_M & , & \dot{\theta}_T &=& a_T/V_T \end{array} \tag{1}$$

where $(x_M\ ,\ x_T)$ and $(y_M\ ,\ y_T)$ are inertial coordinates, V_M and V_T are the velocities, a_{M_t}, a_{M_n} and a_T are the accelerations, and θ_M and θ_T are the flight path angles [Fig. 2]. The subscripts M and T denote the missile and target, respectively, and a_{M_t} and a_{M_n} are tangential and normal accelerations, respectively. Only the normal

A-1

component of the acceleration contributes to changing angular orientations of each vehicle, and the target is assumed to fly at constant speed.

The following target model is assumed to be used in the filter. The objective is to choose a model that is linear in order to reduce the numerical computation of the filter, but reasonably consistent with the nonlinear model so that the estimates are of good quality. The target model for the filter in two dimensions is

$$a_{T_x}(t) = a_T cos(\omega t + \theta), \quad a_{T_y}(t) = a_T sin(\omega t + \theta) \tag{2}$$

where a_T is a constant which is unknown a priori, ω is the angular velocity to be estimated in a right-handed coordinate system, and θ is a Brownian motion process with statistics

$$E[d\theta] = 0, \quad E[d\theta^2] = \Theta dt, \quad \Theta = 1/\tau_\Theta \tag{3}$$

Here, Θ is the power spectral density of the process and τ_Θ is the coherence time, the time for the standard deviation of θ to reach one radian. While in the previous circular target model[4] the acceleration components were just a diffusion process along a circle, those in the new model are related to the actual target motion through a term of physical meaning, ω.

2.2. Dynamic Consistency

In order to see how the current model approximates the assumed nonlinear target dynamics(1), consider a deterministically equivalent case. Integration of (2) with $\Theta = 0$ and $\omega > 0$ yields

$$V_x = \frac{a_T}{\omega} sin\omega t, \quad V_y = -\frac{a_T}{\omega} cos\omega t - V_T + \frac{a_T}{\omega}. \tag{4}$$

where the initial conditions are $V_x = 0$ and $V_y = -V_T$. Adding the square of each component and moving all terms to the left hand side gives

$$2(1 - cos\omega t)[(\frac{a_T}{\omega})^2 - \frac{a_T}{\omega} V_T] = 0. \tag{5}$$

For this equation to hold for all $t \geq 0$

$$\omega = \frac{a_T}{V_T} \tag{6}$$

which is equivalent to the differential equation for angular rate in (1).

Furthermore, by taking the dot product of the velocity vector with the acceleration vector, we obtain

$$\vec{V}_T.\vec{a}_T = a_T[-V_T + \frac{a_T}{\omega}]sin\omega t = 0 \tag{7}$$

using (6) for all $t \geq 0$. This orthogonality between target velocity and acceleration demonstrates the dynamic consistency of the proposed target acceleration model for the filter with the nonlinear target dynamics.

3. New Dynamic and Measurement Models for Estimation

The previous section dealt with a new circular model for filter implementation in order to exploit an assumed characterization of the motion of a typical target. In this section, the stochastic dynamic equations for the new target model are derived. Furthermore, the kinematic fictitious measurement suggested in [7,8] is also discussed.

3.1. Formulation and Approximation

Itô stochastic calculus[12] applied to the Eq.(2) results in a stochastic differential equation with white state-dependent noise[9].

$$\begin{bmatrix} da_{T_x} \\ da_{T_y} \end{bmatrix} = \begin{bmatrix} -\frac{\Theta}{2} & -\omega \\ \omega & -\frac{\Theta}{2} \end{bmatrix} \begin{bmatrix} a_{T_x} \\ a_{T_y} \end{bmatrix} dt + \begin{bmatrix} 0 & -d\theta \\ d\theta & 0 \end{bmatrix} \begin{bmatrix} a_{T_x} \\ a_{T_y} \end{bmatrix} \tag{8}$$

where the elements $-\frac{\Theta}{2}$ in the drift coefficient are the Itô correction terms. Note that the problem is nonlinear due to the unknown ω. To avoid solving the nonlinear problem, ω is approximately removed by an expansion of state variables as in [10]. Define new states as

$$\begin{array}{rclcrcl} a_x^1 & = & \omega a_x & , & a_x^2 & = & \omega a_x^1 \ , \ \ldots \\ a_y^1 & = & \omega a_y & , & a_y^2 & = & \omega a_y^1 \ , \ \ldots \end{array} \tag{9}$$

with the assumption

$$|\omega| = |\frac{a^{i+1}}{a^i}| \ll 1. \tag{10}$$

By augmenting the dynamics of these new states to (2), an approximate dynamical

model which includes this new target model is truncated as

$$\begin{bmatrix} da_x \\ da_y \\ da_x^1 \\ da_y^1 \\ \cdot \\ \cdot \\ da_x^i \\ da_y^i \end{bmatrix} = \begin{bmatrix} -\frac{\Theta}{2} & 0 & 0 & -1 & 0 & 0 \\ & -\frac{\Theta}{2} & 1 & 0 & 0 & 0 \\ & & -\frac{\Theta}{2} & 0 & 0 & -1 \\ & & & -\frac{\Theta}{2} & 1 & 0 \\ & \text{zero} & & & -\frac{\Theta}{2} & 0 \\ & \text{elements} & & & & \\ & & & & & -\frac{\Theta}{2} \end{bmatrix} \begin{bmatrix} a_x \\ a_y \\ a_x^1 \\ a_y^1 \\ \cdot \\ \cdot \\ a_x^i \\ a_y^i \end{bmatrix} + \begin{bmatrix} -a_y \\ a_x \\ -a_y^1 \\ a_x^1 \\ \cdot \\ \cdot \\ -a_y^i \\ a_x^i \end{bmatrix} d\theta \qquad (11)$$

Note that ω does not appear explicitly in (11), and (11) is a linear stochastic differential equation. An idea of this sort, given in [10] for a scalar problem, led to significantly improved filter performance.

3.2. Two-dimensional Intercept

The two dimensional intercept problem is developed in a relative inertial coordinate system. The system dynamics are expressed in the following set of equations:

$$\begin{array}{llll} \dot{x}_r = u_r, & & \dot{y}_r = v_r, & \\ \dot{u}_r = a_{T_{x_r}} - a_{M_{x_r}}, & & \dot{v}_r = a_{T_{y_r}} - a_{M_{y_r}}, & \\ a_{T_{x_r}} = a_T cos(\omega t + \theta), & & a_{T_{y_r}} = a_T sin(\omega t + \theta). & \end{array} \qquad (12)$$

With the assumption of $\omega \ll 1$ and truncation of the target dynamics up to the second order, the ten-element state vector is defined as

$$\begin{aligned} x &\equiv [\ x_r\ \ y_r\ \ u_r\ \ v_r\ \ a_x\ \ a_y\ \ a_x^1\ \ a_y^1\ \ a_x^2\ \ a_y^2\ \ ]^T \\ &= [\ x_1\ \ x_2\ \ x_3\ \ x_4\ \ x_5\ \ x_6\ \ x_7\ \ x_8\ \ x_9\ \ x_{10}\ \ ]^T. \end{aligned} \qquad (13)$$

Thus, in terms of the expanded state space, the linear, stochastic state differential equation is described by

$$dx = (Fx + Bu)dt + Gd\theta \qquad (14)$$

where F is given by the relations in (12) and by the coefficient matrix of x in (11) where $i = 2$, B is a 10×2 matrix of zero except for $B_{31} = B_{42} = -1$, $u = (a_{M_{x_r}}, a_{M_{y_r}})^T$, and

$$G = [\ 0\ \ 0\ \ 0\ \ 0\ \ -x_6\ \ x_5\ \ -x_8\ \ x_7\ \ -x_{10}\ \ x_9\ ]^T. \qquad (15)$$

3.3. Measurement

Angle measurement

Angle information in discrete-time is assumed. Then, the measurement at time t_k is

$$z_1(t_k) = h_1(x(t_k)) + v_k = tan^{-1}(y_r/x_r) + v_k \tag{16}$$

where v_k is a white random sequence with statistics

$$E[v_k] = 0, \;\; E[u_k v_l^T] = V_1 \delta_{kl}. \tag{17}$$

Fictitious measurement

In Ref.[7,8] the filter performance is improved by introducing a kinematic constraint based on a priori knowledge, which is implemented in the form of an augmented fictitious measurement. In particular, the acceleration vector is assumed to be related to the velocity as

$$\vec{V}_T \cdot \vec{a}_T \;\; = \;\; 0 \tag{18}$$

under the assumption that the target accelerates predominantly orthogonally to its velocity vector. When this condition is not met, the acceleration has a component in the direction of the target velocity as

$$\vec{V}_T \cdot \vec{a}_T \;\; = \;\; \eta \tag{19}$$

where $\vec{V}_T$ and $\vec{a}_T$ are assumed to be random vectors representing target velocity and acceleration, and η is the uncertainty in the orthogonality. This idea can be implemented in the form of a discrete pseudo-measurement as

$$\begin{aligned} z_2(t_k) &= h_2(x(t_k)) + \eta_k \\ &= V_{T_{x_r}} a_{T_{x_r}} + V_{T_{y_r}} a_{T_{y_r}} + \eta_k \end{aligned} \tag{20}$$

where η_k is a white random sequence with assumed statistics

$$E[\eta_k] = 0, \;\; E[\eta_k \eta_l^T] = V_2 \delta_{kl}. \tag{21}$$

Note that the variance of the measurement noise corresponds to the tightness of the constraint. In other words, the larger the variance, the more relaxed are the requirements on longitudinal acceleration. This fictitious measurement is used along with the angle measurement in the modified gain extended Kalman filter described in the next section.

4. Estimation of Target States

In this section, the modified gain extended Kalman filter(MGEKF)[11] is derived for the circular target model and for the fictitious and angle measurement defined in the previous section. Also, considered is the method to reconstruct the maneuver rate using the estimated states. Given the continuous-time dynamics and discrete-time measurements, as in the previous section, construction of the filter is completed by specifying the time propagation and measurement update procedures.

4.1 Time Propagation

The state estimate $\bar{x}(t/t_{i-1})$is propagated from the current time t_{i-1} to the next sample time t_i by integrating

$$\begin{array}{lcl} \dot{\bar{x}}(t/t_{i-1}) & = & F\bar{x}(t/t_{i-1}) + Bu(t), \\ \dot{\bar{P}}(t/t_{i-1}) & = & F\bar{P}(t/t_{i-1}) + \bar{P}(t/t_{i-1})F^T + E[G\Theta G^T], \\ \dot{X}(t) & = & FX(t) + X(t)F^T + E[G\Theta G^T]. \end{array} \tag{22}$$

given the posteriori estimate $\bar{x}(t_{i-1}/t_{i-1}) = \hat{x}(t_{i-1})$ and posteriori pseudo-error variance $\bar{P}(t_{i-1}/t_{i-1}) = P(t_{i-1})$. The notation $R(t/t_{i-1})$ denotes the value of some quantity R at time t given the measurement sequence up to time t_{i-1}. The integration of the covariance of the state $X(t)$ begins with $X(0)$ at time $t = 0$. Upon integrating the equations above to the next sample time, the propagated estimates are obtained as follows:

$$\bar{x}(t_i) = \bar{x}(t_i/t_{i-1}), \quad \bar{P}(t_i) = \bar{P}(t_i/t_{i-1}) \tag{23}$$

It should be noted that since the process noise is state-dependent , the integration to propagate $\dot{\bar{P}}(t)$ also requires the integration of $\dot{X}(t)$, where $E[G\Theta G^T]$ matrix turns out to have nonzero elements for its lower-right 6×6 matrix. Note that the approximation technique reduces the originally nonlinear dynamics to linear dynamics. This

allows for the closed form solutions of the propagation of the estimates rather than performing on-line integration.

4.2 Measurement Update[11]

The states are updated as follows:

$$\begin{aligned} \hat{x}(t_i) &= \bar{x}(t_i) + K(t_i)[z - h(\bar{x}(t_i))], \\ K(t_i) &= \bar{P}(t_i)H(t_i)^T[H(t_i)\bar{P}(t_i)H^T(t_i) + V]^{-1} \end{aligned} \tag{24}$$

where $V = \begin{bmatrix} V_1 & 0 \\ 0 & V_2 \end{bmatrix}$ and

$$\begin{aligned} \frac{\partial h}{\partial x}|_{x(t_i)=\bar{x}(t_i)} &\triangleq H(t_i) \\ &= \begin{bmatrix} H_{11}, & H_{12}, & 0, & 0, & ,0, & .., & ...., & 0 \\ 0, & 0, & H_{23}, & H_{24}, & H_{25}, & H_{26}, & ... & 0 \end{bmatrix} \end{aligned} \tag{25}$$

with

$$H_{11} = -\frac{\bar{y}_r}{\bar{x}_r^2 + \bar{y}_r^2}, \quad H_{12} = \frac{\bar{x}_r}{\bar{x}_r^2 + \bar{y}_r^2},$$
$$H_{23} = \bar{x}_5, \quad H_{24} = \bar{x}_6, \quad H_{25} = \bar{x}_3 + V_{x_M}, \quad H_{26} = \bar{x}_4 + V_{y_M}$$

where the missile acceleration in the x and y directions, a_{M_x} and a_{M_y}, are assumed to be measured very accurately with on-board sensors.

The measurement update of the pseudo-error variance is performed by

$$\begin{aligned} P(t_i) &= [I - K(t_i)g(z(t_i), \bar{x}(t_i))]\bar{P}(t_i)[I - K(t_i)g(z(t_i), \bar{x}(t_i))]^T \\ &\quad + K(t_i)R(t_i)K(t_i)^T \end{aligned} \tag{26}$$

where $g(z(t_i), \bar{x}(t_i))$ is used in the update of P rather than H of Eq. (25) and is given as

$$\begin{aligned} h(x(t_i)) - h(\bar{x}(t_i)) &= \begin{bmatrix} tan^{-1}\frac{y_r(t_i)}{x_r(t_i)} - tan^{-1}\frac{\bar{y}_r(t_i)}{\bar{x}_r(t_i)} \\ h_2(x(t_i)) - h_2(\bar{x}(t_i)) \end{bmatrix} \\ &= g(z(t_i), \bar{x}(t_i))(x(t_i) - \bar{x}(t_i)) \end{aligned} \tag{27}$$

Note that g is a 2×10 matrix of function explicit only in the known quantities z and $\bar{x}$. In this sense, the function h has a universal linearization with respect to

the measurement function z. Unfortunately, this type of linearization with respect to the measurements occurs for only a few functions. It is applicable to angle measurements[11], but not for our new pseudo-measurement. Therefore, we must for the pseudo-measurement revert back to the extended Kalman filter form and define

$$\begin{aligned} g_2(z(t_i), \bar{x}(t_i)) &= h_2(x(t_i)) - h_2(\bar{x}(t_i)) \\ &= \frac{\partial h_2}{\partial x(t_i)}|_{x=\bar{x}}(x(t_i) - \bar{x}(t_i)) \end{aligned} \tag{28}$$

where the expression for $\frac{\partial h_2}{\partial x(t_i)}|_{x=\bar{x}}$ is found in the second row of H in (25)

For angle measurements[11]

$$\begin{aligned} h_1(x(t_i)) - h_1(\bar{x}(t_i)) &= g_1(z(t_i), \bar{x}(t_i))(x(t_i) - \bar{x}(t_i)) \\ &= -E(t_i)\bar{H}(t_i)(x(t_i) - \bar{x}(t_i)) \end{aligned} \tag{29}$$

where

$$\begin{aligned} E(t_i) &= \frac{D(t_i)tan^{-1}\alpha(t_i)}{\alpha(t_i)} \\ D(t_i) &= \frac{\sqrt{x_r(t_i)^2 + y_r(t_i)^2}}{(x_r(t_i)\bar{x}_r(t_i) + y_r(t_i)\bar{y}_r(t_i))} \\ \alpha(t_i) &= D(t_i)\bar{H}(t_i)(z^*(t_i))\bar{x}(t_i) \\ \bar{H}(z(t_i)) &= [sin\ z(t_i),\ \ , -cos\ z(t_i)\ , 0\ , 0\ , 0\ , ...] \end{aligned} \tag{30}$$

As discussed in [11], $g(z(t_i), \bar{x}(t_i))$ is only used in the update of $P(t_i)$ but not in the gain, since it was empirically shown that this procedure leads to an unbiased estimate of the state.

4.3. Estimation of ω and T_{go}

Since the target angular velocity term is embedded in the states, ω should be reconstructed using the estimated states. A simple way to determine the value of ω is to divide the states as $\omega = \frac{a_x^1}{a_x}$ *or* $\frac{a_x^2}{a_x^1}$. However, since the expanded state space is originally an approximated state space, this might lead to numerical errors, especially when the higher approximated terms are used. By relying on the definition of the

vector relation between and velocity and acceleration, the target angular velocity can be obtained without using the augmented states for approximation. From the assumed dynamics the target angular velocity during its evasive maneuver is

$$\vec{\omega}_T = \frac{\vec{V}_T \times \vec{a}_T}{|\vec{V}_T|^2} \tag{31}$$

Thus, by using the state estimates, ω is constructed as

$$\hat{\omega} = sign(\hat{V}_{T_x}\hat{a}_{T_y} - \hat{V}_{T_y}\hat{a}_{T_x})|\frac{\hat{a}_T}{\hat{V}_T}| \tag{32}$$

To be used later in the controller, an estimate of time-to-go, T_{go}, is required, and approximated here as

$$\hat{T}_{go} = \frac{\hat{R}}{|\dot{\hat{R}}|} = \frac{\hat{R}}{|\hat{X} \cdot \hat{V}|/\hat{R}} \tag{33}$$

where $\hat{R}$ and $\dot{\hat{R}}$ are the estimates of relative range and range rate, respectively, and the vectors $\hat{X}$ and $\hat{V}$ are the estimates of relative position and velocity, respectively.

5. Linear Quadratic Guidance Law

Based on the estimated states and the estimate of the rotation rate constructed from the estimated states, a guidance law can be mechanized. In the following, a stochastic guidance law is determined which minimizes a quadratic performance index subject to the stochastic engagement dynamics including the stochastic circular target model(8) under the assumption that states including the target states and the target rotation rate are known perfectly. This assumption simplifies the derivation of the guidance law enormously, and for this homing problem it is shown that the solution to the stochastic control problem with state-dependent noise can be obtained in closed form. The solution obtained does not produce a certainty equivalence controller since the guidance law explicitely depends upon the system statistics.

Note that since the noise in each cartesian direction is correlated in the stochastic circular target model(8), and that with a_{T_x} and a_{T_y} dynamically coupled through ω

term, the guidance commands in the x and y direction cannot be achieved independently. Thus, the optimal stochastic controller for circular target model is based on the minimization of the performance index

$$J = E\{\frac{1}{2}[x_f^2 + y_f^2] + \frac{c}{2}\int_0^{t_f}[a_{M_x}^2 + a_{M_y}^2]dt\} \tag{34}$$

subject to the following stochastic system of linear dynamic equations

$$\begin{aligned} dx &= u dt \\ dy &= v dt \\ du &= (a_{T_x} - a_{M_x})dt \\ dv &= (a_{T_y} - a_{M_y})dt \\ da_{T_x} &= (-\frac{\Theta}{2}a_{T_x} - \omega a_{T_y})dt - a_{T_y}d\theta \\ da_{T_y} &= (-\frac{\Theta}{2}a_{T_y} + \omega a_{T_x})dt + a_{T_x}d\theta \end{aligned} \tag{35}$$

where θ is a Brownian motion defined earlier and $E[\cdot]$ stands for an expectation operator. In the construction of filter, the inherent nonlinearity of the target model was removed by an expansion of state variables. However, for the guidance law formulation, the rotation rate, ω, is assumed known, although it must be constructed on-line from the state estimator(32).

For brevity of notation, define the state and control vectors as follows :

$$\begin{aligned} \boldsymbol{x} &\triangleq [x, y, u, v, a_{T_x}, a_{T_y}]^T \\ \boldsymbol{u} &\triangleq [a_{M_x}, a_{M_y}]^T \end{aligned} \tag{36}$$

Then, the stochastic control problem is to find $\boldsymbol{u}$ which minimizes

$$J = E\{\frac{1}{2}\int_0^{t_f} \boldsymbol{u}^T R \boldsymbol{u} d\tau + \frac{1}{2}\boldsymbol{x}_f^T S_f \boldsymbol{x}_f\} \tag{37}$$

subject to the stochastic differential equation with state dependent noise

$$d\boldsymbol{x} = [A\boldsymbol{x} + B\boldsymbol{u}]dt + D(\boldsymbol{x})d\theta \tag{38}$$

where

$$A = \begin{bmatrix} 0 & 0 & 1 & 0 & 0 & 0 \\ 0 & 0 & 0 & 1 & 0 & 0 \\ 0 & 0 & 0 & 0 & 1 & 0 \\ 0 & 0 & 0 & 0 & 0 & 1 \\ 0 & 0 & 0 & 0 & -\frac{\Theta}{2} & -\omega \\ 0 & 0 & 0 & 0 & \omega & -\frac{\Theta}{2} \end{bmatrix}, B = \begin{bmatrix} 0 & 0 \\ 0 & 0 \\ 1 & 0 \\ 0 & 1 \\ 0 & 0 \\ 0 & 0 \end{bmatrix} \tag{39}$$

$$D(\underline{x}) = \begin{bmatrix} 0 \\ 0 \\ 0 \\ 0 \\ -x_6 \\ x_5 \end{bmatrix}, R = c \begin{bmatrix} 1 & 0 \\ 0 & 1 \end{bmatrix}, S_f = \begin{bmatrix} 1 & 0 & 0 & 0 & 0 & 0 \\ & 1 & 0 & 0 & 0 & 0 \\ & & 0 & 0 & 0 & 0 \\ & & & 0 & 0 & 0 \\ & & & & 0 & 0 \\ & & & & & 0 \end{bmatrix}$$

where $c > 0$. Note that

$$D(x) = \sum_{j=1}^{6} x_j D_j, \quad D_j \in R^{6\times 1} \tag{40}$$

where x_j is the j^{th} element of x and where

$$D_1, D_2, D_3, D_4 = \begin{bmatrix} 0 \\ 0 \\ 0 \\ 0 \\ 0 \\ 0 \end{bmatrix}, D_5 = \begin{bmatrix} 0 \\ 0 \\ 0 \\ 0 \\ 0 \\ 1 \end{bmatrix}, D_6 = \begin{bmatrix} 0 \\ 0 \\ 0 \\ 0 \\ -1 \\ 0 \end{bmatrix} \tag{41}$$

To obtain an optimal control for this class of problem, dynamic programming[13,14] is employed where the Hamilton-Jacobi-Bellman equation becomes

$$0 = J_t^o(x,t) + \underset{u}{Min}\{J_x^o(Ax + Bu) + \frac{1}{2}[x^T \Delta(J_{xx}^o, t)x + u^T Ru]\} \tag{42}$$

where J^o is the optimal return function and the subscripts denote partial derivatives. The elements of the matrix Δ for any symmetric matrix W is defined as

$$\Delta_{ij}(W,t) = tr[D_i(t)^T W D_j(t)] \tag{43}$$

The minimization operator in (25) produces

$$u = -R^{-1}B^T J_x^o \tag{44}$$

By substituting (44) into (42), the dynamic programming equation becomes

$$0 = J_t^o + J_{\boldsymbol{x}}^o A\boldsymbol{x} - \frac{1}{2} J_{\boldsymbol{x}}^o B R^{-1} B J_{\boldsymbol{x}}^o + \frac{1}{2}\boldsymbol{x}^T \Delta(J_{\boldsymbol{xx}}^o, \Theta, t)\boldsymbol{x} \tag{45}$$

The optimization problem is solved by explicitely showing that the equation above has a solution . Asume $J^o(\boldsymbol{x}, t) = \frac{1}{2}\boldsymbol{x}^T S(t)\boldsymbol{x}$, then

$$J_t^o = \frac{1}{2}\boldsymbol{x}^T \dot{S}\boldsymbol{x}, \;\; J_{\boldsymbol{x}}^o = \boldsymbol{x}^T S, \;\; J_{\boldsymbol{xx}}^o = S \tag{46}$$

With this assumption, the dynamic programming equation is satisfied for all $\underline{x} \in R^n$ if

$$\dot{S} + SA + A^T S + \Delta - SBR^{-1}B^T S = 0, \;\; S(t_f) = S_f \tag{47}$$

The desired optimal controller becomes

$$\boldsymbol{u} = -R^{-1}B^T S\boldsymbol{x} \tag{48}$$

where S is the solution of the Riccati equation and the $\Delta(S,t)_{ij} = tr[D_i^T S D_j]$ leads to

$$\Delta = \begin{bmatrix} \text{zero} & & \\ \text{elements} & & \\ & S_{66} & -S_{56} \\ & -S_{56} & S_{55} \end{bmatrix} \tag{49}$$

The fact that Δ has only nonzero elements for its lower-right 2×2 matrix allows a tractable closed-form solution. To see the characteristics of the solution in a simple manner, matrices are partition such that their lower-right block partitioned is a 2×2 matrix. Then

$$A = \begin{bmatrix} A_{11} & A_{12} \\ 0 & A_{22} \end{bmatrix}, B = \begin{bmatrix} B_1 \\ 0 \end{bmatrix}, S = \begin{bmatrix} S_{11} & S_{12} \\ S_{12}^T & S_{22} \end{bmatrix}, \Delta = \begin{bmatrix} 0 & 0 \\ 0 & \tilde{S} \end{bmatrix} \tag{50}$$

where $\tilde{S}$ is defined in (49). This leads to the controller of (48)

$$\boldsymbol{u} = \begin{bmatrix} a_{M_z} \\ a_{M_y} \end{bmatrix} = -\frac{1}{c}\begin{bmatrix} B_1^T S_{11} \\ B_1^T S_{12} \end{bmatrix}\boldsymbol{x} \tag{51}$$

where the block matrices satisfies the decomposed Riccati equation

$$\begin{aligned} -\dot{S}_{11} &= S_{11}A_{11} + A_{11}^T S_{11} - S_{11}B_1 R^{-1} B_1^T S_{11} \\ -\dot{S}_{12} &= S_{11}A_{12} + S_{12}A_{22} + A_{11}^T S_{12} - S_{11}B_1 R^{-1} B_1^T S_{12} \\ -\dot{S}_{22} &= S_{12}A_{12} + S_{22}A_{22} + A_{22}^T S_{22} + A_{12}^T S_{22} + \tilde{S} - S_{12}B_1 R^{-1} B_1^T S_{12} \end{aligned} \tag{52}$$

Since the S_{22} block does not affect the block matrices S_{11} and S_{12}, the optimal control law is not dependent on S_{22}. Therefore, the closed form optimal guidance law for this special class of problem can be obtained by integrating the Riccati equation backwards without requiring the explicit evaluation of the Δ term. In particular, the stochastic optimal control problem essentially degenerates to a deterministic optimal control problem although the Itô terms are retained. The solution process for this deterministic control problem, explained in detail in the Appendix A, produces a guidance law in closed form. Note that the deterministic coefficient A_{22} includes the statistic Θ. Therefore, the resulting controller is not a certainty equivalence controller. The new controller becomes

$$\begin{bmatrix} a_{M_x} \\ a_{M_y} \end{bmatrix} = \begin{bmatrix} c_1 & 0 & c_2 & 0 & c_3 & c_4 \\ 0 & c_1 & 0 & c_2 & -c_4 & c_3 \end{bmatrix} \begin{bmatrix} x(t) \\ y(t) \\ u(t) \\ v(t) \\ a_{T_x}(t) \\ a_{T_y}(t) \end{bmatrix} \tag{53}$$

where the gains c_1 to c_4 are an explicit function of T_{go}, ω, and Θ as

$$\begin{aligned} c_1 &= \frac{T_{go}}{c + \frac{T_{go}^3}{3}}, \quad c_2 = \frac{T_{go}^2}{c + \frac{T_{go}^3}{3}} \\ c_3 &= c^* \{ \frac{\Theta T_{go}}{2} e^{\frac{\Theta}{2} T_{go}} - sin\omega T_{go} \frac{\omega\Theta}{(\frac{\Theta^2}{4} + \omega^2)} + (cos\omega T_{go} - e^{\frac{\Theta}{2} T_{go}}) \frac{(\frac{\Theta^2}{4} - \omega^2)}{(\frac{\Theta^2}{4} + \omega^2)} \} \\ c_4 &= c^* \{ -\omega T_{go} e^{\frac{\Theta}{2} T_{go}} + (e^{\frac{\Theta}{2} T_{go}} - cos\omega T_{go}) \frac{\omega\Theta}{(\frac{\Theta}{4} + \omega^2)} - sin\omega T_{go} \frac{(\frac{\Theta^2}{4} - \omega^2)}{(\frac{\Theta^2}{4} + \omega^2)} \} \end{aligned} \tag{54}$$

where $c^* = \dfrac{T_{go}}{e^{\frac{\Theta}{2} T_{go}} (c + \frac{T_{go}^3}{3})(\frac{\Theta^2}{4} + \omega^2)}$.

Fig. 1 is a block diagram for an adaptive guidance scheme for a homing missile. Note that guidance gains are functions of $\hat{T}_{go}$, estimated time to go, the statistic Θ and the estimated maneuver rate $\hat{\omega}$. Therefore, for the bearing-only measurement system although the resulting stochastic guidance law is sub-optimal since the measurements are nonlinear functions of the states, the explicit dependence on the estimate of the target maneuver rate is a new feature which should help reduce terminal miss distance.

6. Numerical Simulation

For a particular engagement scenario, the performance of the estimator using the new target models and that of the guidance law are evaluated.

6.1. Missile and Target model

Both target and missile are treated as point masses and are considered in two-dimensional reference frames as shown in Fig. 2. The missile represents a highly maneuverable, short range air-to-air missile with a maximum normal acceleration of $100g's$. It is launched with a velocity $M = 0.9$ at a $10,000ft$ altitude with zero normal acceleration. After a 0.4 sec delay to clear the launch rail, it flies by the guidance command provided by the linear quadratic guidance law of Section 5. Also, to compensate for the aerodynamic drag and propulsion, the missile is modeled to have a known longitudinal acceleration profile : $a_M = 25g's$ for $t \leq 2.6sec$, $a_M = -15g's$ for $t > 2.6sec$. The target model flies at a constant speed of $M = 0.9$, and at an altitude of $10,000ft$. It accelerates at 9 $g's$ either at the beginning or in the middle of the engagement.

The actual states are first used in the guidance law to produce consistency in evaluating the performance of the filter. In evaluating the actual miss distances, the filter state estimates are used in the guidance law. Two engagements, considered in the following section, are shown in Fig. 3. With R_i and R_M denoting initial range and maneuver onset range, respectively, engagement 1 is the situation where the target maneuver starts at the beginning, and for engagement 2 the maneuver starts in the middle.

6.2. Filter Parameters and Initial conditions

Integration of actual trajectories is performed by a fourth-order Runge-Kutta integrator with step size 0.02 seconds. The variance for the angle measurement is chosen, as given in [4], to be

$$V_1 = a\, V_o\,, \quad V_0 = (\frac{0.25}{R^2} + 5.625 * 10^{-7})/\Delta t \qquad rad^2 \tag{55}$$

where R is range, Δt is filter sample time, and a is parameter which is used in the simulation indicating different levels of sensor accuracy.

As mentioned earlier, the variance for the pseudo-measurement can be interpreted to show how strictly the orthogonality assumption between the target velocity and acceleration is to be kept. By allowing some acceleration in the longitudinal direction, a reasonable estimate of the variance to be used can be given. Suppose that the acceleration component in the velocity direction has a normal distribution with zero mean. Then with probability 0.95, a 1 g acceleration while flying with $V_T = 970 ft/sec$ leads to $2\,\sigma = 3.12 * 10^4\ [ft^2/sec^3]$, where σ is the standard deviation, which results in a variance $V_2 = 2.44 * 10^8\ [ft^2/sec^3]^2$.

Unless otherwise stated the filter is initialized at launch with the true relative position and relative velocity component values. Hence, the initial values for the diagonal elements of the covariance matrix associated with position and velocity, P_{11}, P_{22}, P_{33}, and P_{44} are set to ten. On the other hand, little knowledge about target acceleration is assumed to be provided at the beginning. Therefore, the initial values for the target acceleration and expanded states are zero. Initial values of the covariance matrix associated with target acceleration is calculated by resorting to the definition of the target acceleration at $t = 0$ given in (2). Those covariances are produced in the Appendix B. The target is expected to execute a maximum acceleration turn in its evasive motion, and the missile has no knowledge about the direction of target rotation. Note that θ is a Brownian motion process beginning at $\theta(0) = \bar{\theta}$, the expected angle the target acceleration vector makes with respect to the x_r axis at the time of launch, and $a_{T_{max}}$ is the expected maximum acceleration of

target. For the simulation with a coordinate system having one axis perpendicular to the initial V_T direction, $\bar{\theta}$ is zero. Then, the possible nonzero elements of the upper triangular part of the initial covariance matrix are $P_{55}(0)$, $P_{57}(0)$, $P_{59}(0)$, $P_{77}(0)$, $P_{79}(0)$, and $P_{99}(0)$. Furthermore, no information is available about the direction of maneuver, and the possible maximum rotation rate can be either positive or negative. Thus, the odd powers of $\bar{\omega}$ are taken as zero. This leaves only $P_{55}(0)$, $P_{59}(0)$, $P_{77}(0)$, $P_{99}(0)$ as the nonzero elements. However, a value of ten is assigned to P_{66}, P_{88}, and $P_{10\,10}$ to ensure positive definiteness of the covariance matrix at the initial time.

6.4. Filter Results

The results in this section are the product of a Monte Carlo analysis consisting of ten filter runs. Along with the miss distance calculations, the plots of the estimation error and the ω estimates versus time are mainly considered. The errors are calculated as $[E[e_x]^2 + E[e_y]^2]^{1/2}$ where $E[e_x]$ and $E[e_y]$ are the averaged values of errors over ten simulation runs.

Figs. 4-5 represents the results for the engagement 1 where the target maneuver initiates at $t = 0$ and the pseudo-measurement is not used. As seen in Fig. 4, when there is no switching of the direction of the target acceleration during the maneuver, the estimation results get better as the power spectral density of the process noise decreases. When Θ is relatively large, the target acceleration estimation is poor, and divergence of the position and velocity estimation occurs. This causes the estimate of ω to deteriorate as time goes on. However, with small Θ, the filter performance improves considerably. As shown in Fig. 5, estimation improves with better angle measurements.

When the auxiliary pseudo-measurement is also implemented in the filter, estimation performance improves over the case when only an angle measurement is used. This is shown in Fig. 6 where again the target starts its acceleration maneuver at the beginning of the engagement($R_i = R_M$). At first, the filter with the fictitious measurement seems to work a little worse than the filter with angle-only measurement. Then, the fictitious measurement promptly works as if it suppressed or delayed

the filter divergence. Note that the effect of two values of pseudo-noise variance are shown.

The role of the fictious measurement is more observable for engagement 2 where the target maneuver begins in the middle of the angagement($R_M = 4000ft$). As plotted in Fig. 7, the filter equipped with only the angle measurement diverges as soon as the target maneuver occurs. On the other hand, when the filter is augmented with the fictitious measurement, it works very effectively. The divergence of position and velocity is noticeably suppressed, and the acceleration estimate tend to return to its actual value from an instantaneous large acceleration error. With the accuracy of the angle measurement increased, the target acceleration estimate after the maneuver onset improves faster than the filter that uses poor angle measurements. This is shown in Fig. 8. However, after the target started to maneuver in the middle of the engagement, position and velocity error estimates do not reduce as V_1 becomes smaller.

Miss distances have been calculated on the basis of 50 runs of Monte Carlo simulations with an approximate error ± 0.02 ft due to subdiscretization near the final time. In the Table 1, the actual states are fed to the guidance law in the Case I, and the estimated states and maneuver rate estimate are fed to the guidance law in the Case II and III. The estimates are obtained from angle-only measurements in the Case II, and from both angle and pseudo-measurement in the Case III. Miss distance performance is tested as more noise is introduced into the measurement and then into the dynamics. For the particular scenario chosen here, miss distance has been improved by using the angle and pseudo-measurement, especially as the process noise power spectral density Θ in the state dependent noise term decreases.

7. Conclusions

The orthogonality between the target acceleration and velocity vectors is a typical characteristic of the target of an air-to-air missile, and it is utilized in the development of a new stochastic target acceleration model for the homing missile problem.

In addition, this characteristic is also implemented in the form of an augmented pseudo-measurement. A guidance law that minimizes a quadratic performance index subject to the stochastic engagement dynamics is determined in closed form where the gains are an explicit function of the estimated target maneuver rate and time to go. Preliminary results for the two-dimensional case indicates that the circular target model is able to produce a reliable estimate in the homing missile engagement. When it is augmented by the fictitious measurement, the modified gain extended Kalman filter using the proposed target model results in the remarkable enhancement of target state estimation for both a maneuvering and nonmaneuvering situation. This is because the circular target model inherently includes a better approximation to the simulation dynamics of target motion, and the pseudo-measurement imposes satisfaction of the orthogonality characteristic through the measurement process. However, the improvement in miss distance for a particular engagement shows significant improvement in going from angle-only measurement to both angle measurement and pseudo-measurement when the process uncertainty decreases.

Acknowledgements

This work was supported by the Air Force Armament Laboratory, Eglin AFB, under contract FO8635-87-K-0417.

References

1. Chang, C.B. and Tabsczynsky, J. A.,"Application of State Estimation to Target Tracking," *IEEE Trans. Automat. Contr.*, Vol. AC-29, No.2, Feb., 1984

2. Lin, C. F. and Shafroth, M. W., "A Comparative Evaluation of some Maneuvering Target Tracking Algorithms," *Proceedings of AIAA Guidance and Control Conference*, 1983

3. Vergez, P. L. and Liefer, R. K., "Target Acceleration Modeling for Tactical Missile Guidance," *AIAA J. of Guidance and Control*, Vol.7, No.3, May-June 1984

4. Hull, D. G., Kite, P. C. and Speyer, J. L., "New Target Models for Homing Missile Guidance," *Proceedings of AIAA Guidance and Control Conference*, 1983

5. Berg, R. F., "Estimation and Prediction for Maneuvering Target Trajectories," *IEEE Trans. Automat. Contr.*, Vol. AC-28, No. 3, Mar., 1983

6. Song, T. L., Ahn, J. Y., and Park, C., "Suboptimal Filter Design with Pseudomeasurements for Target Tracking," *IEEE Trans. Aerospace and Electronics*, Vol. 24, No. 1, Jan. 1988

7. Tahk, M. J. and Speyer, J. L., "Target Tracking Problems subject to Kinematic Constraints," Proceedings of the *27th IEEE Conf. on Decision and Control*, Dec. 1988

8. Kim, K. D., Speyer, J. L. and Tahk, M., "Target Maneuver Models for Tracking Estimators," Proceedings of the *IEEE International Conference on Control and Applications, April, 1989*

9. Gustafson, D. E. and Speyer, J. L.,"Linear Minimum Variance Filters Applied to Carrier Tracking," *IEEE Trans. Automat. Contr.*, Vol. AC-21, No.1, Feb. 1976

10. Speyer, J. L. and Gustafson, D. E.,"An Approximation Method for Estimation in Linear Systems with Parameter Uncertainty,"*IEEE Trans. Automat. Contr.*, Vol. AC-20, No. 6, June 1975

11. Song, T. L. and Speyer, J. L., " A Stochastic Analysis of a Modified Gain Extended Kalman Filter with Applications to Estimation with Bearing only Measurements," *IEEE Trans. Automat. Contr.*, Vol. AC-30, No. 10, Oct. 1985

12. Jazwinski, A. H., "Stochastic Process and Filtering Theory," Academic Press, 1970

13. Wonham, W. M., "Random Differential Equations In Control Theory," *Probabilistic Methods in Applied Mathematics*, Vol. 2, Academic Press, 1970

14. Bryson, A. E. and Ho, Y. C.,"Applied Optimal Control Theory," John Wiley & Sons, 1975

Appendix A

2. Linear Quadratic guidance law for deterministic circular target model

In the following, the optimal deterministic guidance law for linear quadratic problem is sought for the current circular target model filter. The deterministic optimal solution can be obtained by solving the Riccati equation without the Δ term via transition matrix approach, but the use of Euler-Lagrange equation seems simpler for this case.

The problem is to minimize the performance index

$$J = \frac{1}{2}[x_f^2 + y_f^2] + \frac{c}{2}\int_t^{t_f}[a_{M_x}^2 + a_{M_y}^2]dt \tag{A-1}$$

subject to the following linear dynamic system

$$\begin{aligned}
\dot{x} &= u \\
\dot{y} &= v \\
\dot{u} &= a_{T_x} - a_{M_x} \\
\dot{v} &= a_{T_y} - a_{M_y} \\
\dot{a}_{T_x} &= -\frac{\Theta}{2}a_{T_x} - \omega a_{T_y} \\
\dot{a}_{T_y} &= -\frac{\Theta}{2}a_{T_y} + \omega a_{T_x}
\end{aligned} \tag{A-2}$$

This linear system of dynamics stems from taking Ito derivative of the corresponding nonlinear stochastic target model (6). The ω is the angular rate of target

maneuver which is handled as a known constant in the derivations. In the actual mechanization of guidance command the value of $\hat{\omega}$ constructed from the estimated states are used.

The variational Hamiltonian and the augmented end-point function are given by

$$\begin{aligned} H &= ca_{M_x}^2 + ca_{M_y}^2 + \lambda_1 u + \lambda_2 v + \lambda_3(a_{T_x} - a_{M_x}) \\ &\quad +\lambda_4(a_{T_y} - a_{M_y}) + \lambda_5(-\frac{\Theta}{2} - \omega a_{T_y}) + \lambda_6(-\frac{\Theta}{2} + \omega a_{T_x}) \end{aligned} \tag{A-3}$$

$$G = \frac{1}{2}(x_f^2 + y_f^2) \tag{A-4}$$

where λ_i , $i = 1, ..., 6$ is a Lagrange multiplier. The Euler-Lagrange equations for λ_i are

$$\dot{\lambda_1} = 0, \quad \dot{\lambda_2} = 0, \quad -\dot{\lambda_3} = \lambda_1, \quad -\dot{\lambda_4} = \lambda_2 \tag{A-5}$$

where the optimal control satisfies the optimality condition

$$a_{M_x} = \frac{\lambda_3}{c}, \quad a_{M_y} = \frac{\lambda_4}{c} \tag{A-6}$$

Finally, the Euler-Lagrange equations with the natural boundary conditions yield

$$\lambda_1 = x_f, \quad \lambda_2 = y_f, \quad \lambda_3 = x_f T_{go}, \quad \lambda_4 = y_f T_{go} \tag{A-7}$$

which gives the control

$$a_{M_x} = x(t_f)T_{go}/c, \quad a_{M_y} = y(t_f)T_{go}/c \tag{A-8}$$

where T_{go} is the time-to-go of missile to intercept the target and c is the guidance law design parameter. In order to get the guidance law in terms of the current states, the underlining dynamics is integrated backward from t_f to t. Succesive integrations of state differential equations yield

$$\begin{aligned} a_{T_x} &= \omega cos\omega T_{go} e^{\frac{\Theta}{2}T_{go}} a_{T_x}(t_f) + \omega sin\omega T_{go} e^{\frac{\Theta}{2}T_{go}} a_{T_y}(t_f) \\ a_{T_y} &= -\omega sin\omega T_{go} e^{\frac{\Theta}{2}T_{go}} a_{T_x}(t_f) + \omega cos\omega T_{go} e^{\frac{\Theta}{2}T_{go}} a_{T_y}(t_f) \\ u &= \frac{1}{2c} T_{go}^2 x(t_f) + u(t_f) \end{aligned}$$

$$
\begin{aligned}
&+\frac{\omega}{\frac{\Theta^2}{4}+\omega^2}[\frac{\Theta}{2}(1-cos\omega T_{go}e^{\frac{\Theta}{2}T_{go}})-\omega sin\omega T_{go}e^{\frac{\Theta}{2}T_{go}}]a_{T_x}(t_f)\\
&+\frac{\omega}{\frac{\Theta^2}{4}+\omega^2}[-\omega(1-cos\omega T_{go}e^{\frac{\Theta}{2}T_{go}})-\frac{\Theta}{2}sin\omega T_{go}e^{\frac{\Theta}{2}T_{go}})]a_{T_y}(t_f)\\
v &= \frac{1}{2c}T_{go}^2y_(t_f)+v(t_f)\\
&+\frac{\omega}{\frac{\Theta^2}{4}+\omega^2}[\omega(1-cos\omega T_{go}e^{\frac{\Theta}{2}T_{go}})+\frac{\Theta}{2}sin\omega T_{go}e^{\frac{\Theta}{2}T_{go}}]a_{T_x}(t_f)\\
&+\frac{\omega}{\frac{\Theta^2}{4}+\omega^2}[\frac{\Theta}{2}(1-cos\omega T_{go}e^{\frac{\Theta}{2}T_{go}})-\omega sin\omega T_{go}e^{\frac{\Theta}{2}T_{go}})]a_{T_y}(t_f)\\
x &= (1-\frac{T_{go}^3}{6c})x(t_f)-T_{go}u(t_f)\\
&+\frac{\omega}{\frac{\Theta^2}{4}+\omega^2}[-\frac{\Theta T_{go}}{2}-\frac{(\frac{\Theta^2}{4}-\omega^2)}{(\frac{\Theta^2}{4}+\omega^2)}(1-cos\omega T_{go}e^{\frac{\Theta}{2}T_{go}})+\frac{\omega\Theta}{(\frac{\Theta^2}{4}+\omega^2)}sin\omega T_{go}e^{\frac{\Theta}{2}T_{go}}]a_{T_x}(t_f)\\
&+\frac{\omega}{\frac{\Theta^2}{4}+\omega^2}[\omega T_{go}+\frac{\omega\Theta}{(\frac{\Theta^2}{4}+\omega^2)}(1-cos\omega T_{go}e^{\frac{\Theta}{2}T_{go}})+\frac{(\frac{\Theta^2}{4}-\omega^2)}{\frac{\Theta^2}{4}+\omega^2}\sin\omega T_{go}e^{\frac{\Theta}{2}T_{go}})]a_{T_y}(t_f)\\
y &= (1-\frac{T_{go}^3}{6c})y(t_f)-T_{go}v(t_f)\\
&+\frac{\omega}{\frac{\Theta^2}{4}+\omega^2}[-\omega T_{go}-\frac{\omega\Theta}{(\frac{\Theta^2}{4}+\omega^2)}(1-cos\omega T_{go}e^{\frac{\Theta}{2}T_{go}})-\frac{(\frac{\Theta^2}{4}-\omega^2)}{(\frac{\Theta^2}{4}+\omega^2)}sin\omega T_{go}e^{\frac{\Theta}{2}T_{go}}]a_{T_x}(t_f)\\
&+\frac{\omega}{\frac{\Theta^2}{4}+\omega^2}[-\frac{\Theta T_{go}}{2}-\frac{(\frac{\Theta^2}{4}-\omega^2)}{\frac{\Theta^2}{4}+\omega^2}(1-cos\omega T_{go}e^{\frac{\Theta}{2}T_{go}})+\frac{\omega\Theta}{\frac{\Theta^2}{4}+\omega^2}sin\omega T_{go}e^{\frac{\Theta}{2}T_{go}}]a_{T_y}(t_f)
\end{aligned}
\tag{A-9}
$$

The final states being expressed in terms of the current states via 6×6 matrix inversion,the optimal guidance law is obtained as equation (53). As expected from dynamic coupling in the target acceleration model, guidance commands in each channel are the function of acceleration components in both x and y directions.

Appendix B

1. State and Error variance associated with target acceleration

Since the initial values for the state estimates associated with target acceleration are set to zero, the state and error variances are computed with the aid of expected

values of trigonometric functions such as

$$E[\cos^2\theta] = \int_{-\infty}^{+\infty} \cos^2\theta p(\theta) d\theta \quad with\ p(\theta) = \frac{1}{\sqrt{2\pi\Theta t}} e^{-(\frac{(\theta-\bar{\theta})^2}{2\Theta t})} \tag{B-1}$$

By using standard manipulation, the expected value of the $\cos^2\theta$ is

$$E[\cos^2\theta] = \frac{1}{2}[1 + cos2\bar{\theta}e^{-2\Theta t}], \tag{B-2}$$

and in the same manner

$$\begin{aligned} E[\sin^2\theta] &= \frac{1}{2}[1 + cos2\bar{\theta}e^{-2\Theta t}], \\ E[\cos\theta\sin\theta] &= \frac{1}{2}\sin 2\bar{\theta}e^{-2\Theta t}. \end{aligned} \tag{B-3}$$

This yeilds the initial conditions for the state and error variances associated with target acceleration as follows.

$$\begin{aligned}
P_{55}(0) = X_{55}(0) &= a^2_{T_{max}}(1 + cos2\bar{\theta})/2, \\
P_{56}(0) = X_{56}(0) &= a^2_{T_{max}} sin2\bar{\theta}/2, \\
P_{57}(0) = X_{57}(0) &= a^2_{T_{max}}\bar{\omega}(1 + cos2\bar{\theta})/2, \\
P_{58}(0) = X_{58}(0) &= a^2_{T_{max}}\bar{\omega} sin2\bar{\theta}/2, \\
P_{59}(0) = X_{59}(0) &= a^2_{T_{max}}\bar{\omega}^2(1 + cos2\bar{\theta})/2, \\
P_{510}(0) = X_{510}(0) &= a^2_{T_{max}}\bar{\omega}^2 sin2\bar{\theta}/2, \\
P_{66}(0) = X_{66}(0) &= a^2_{T_{max}}(1 - cos2\bar{\theta})/2, \\
P_{67}(0) = X_{67}(0) &= a^2_{T_{max}}\bar{\omega} sin2\bar{\theta}/2, \\
P_{68}(0) = X_{68}(0) &= a^2_{T_{max}}\bar{\omega}(1 - cos2\bar{\theta})/2, \\
P_{69}(0) = X_{69}(0) &= a^2_{T_{max}}\bar{\omega}^2 sin2\bar{\theta}/2, \\
P_{610}(0) = X_{610}(0) &= a^2_{T_{max}}\bar{\omega}^2(1 - cos2\bar{\theta})/2, \\
P_{77}(0) = X_{77}(0) &= a^2_{T_{max}}\bar{\omega}^2(1 + cos2\bar{\theta})/2, \\
P_{78}(0) = X_{78}(0) &= a^2_{T_{max}}\bar{\omega}^2 sin2\bar{\theta}/2, \\
P_{79}(0) = X_{79}(0) &= a^2_{T_{max}}\bar{\omega}^3(1 + cos2\bar{\theta})/2, \\
P_{710}(0) = X_{710}(0) &= a^2_{T_{max}}\bar{\omega}^3 sin2\bar{\theta}/2, \\
P_{88}(0) = X_{88}(0) &= a^2_{T_{max}}\bar{\omega}^2(1 - cos2\bar{\theta})/2, \\
P_{89}(0) = X_{89}(0) &= a^2_{T_{max}}\bar{\omega}^3 sin2\bar{\theta}/2, \\
P_{810}(0) = X_{810}(0) &= a^2_{T_{max}}\bar{\omega}^3(1 - cos2\bar{\theta})/2, \\
P_{99}(0) = X_{99}(0) &= a^2_{T_{max}}\bar{\omega}^4(1 + cos2\bar{\theta})/2, \\
P_{910}(0) = X_{910}(0) &= a^2_{T_{max}}\bar{\omega}^4 sin2\bar{\theta}/2, \\
P_{1010}(0) = X_{1010}(0) &= a^2_{T_{max}}\bar{\omega}^4(1 - cos2\bar{\theta})/2,
\end{aligned} \tag{B-4}$$

Table 1

Statistic	Case	$Range_i$ (ft)	$Range_M$ (ft)	Miss Distance(ft)
$\Theta = 0.01$	I	6000	6000	0.35
$V_1 = V_0 \times 10^{-2}$		6000	4000	0.32
$V_2 = 10^6$	II	6000	6000	1.30
		6000	4000	0.74
	III	6000	6000	0.82
		6000	4000	0.54
$\Theta = 0.001$	II	6000	6000	2.65
$V_1 = V_0$		6000	4000	1.71
$V_2 = 10^6$	III	6000	6000	2.13
		6000	4000	1.36
$\Theta = 0.01$	II	6000	6000	4.59
$V_1 = V_0$		6000	4000	1.97
$V_2 = 10^6$	III	6000	6000	4.29
		6000	4000	1.82
$\Theta = 0.1$	II	6000	6000	4.98
$V_1 = V_0$		6000	4000	2.07
$V_2 = 10^6$	III	6000	6000	4.86
		6000	4000	2.01
$\Theta = 0.001$	II	6000	6000	2.65
$V_1 = V_0$		6000	4000	1.71
$V_2 = 10^8$	III	6000	6000	2.34
		6000	4000	1.49

List of Figures

Fig. 1 Diagram of Homing Missile Guidance
Using Circular Target Maneuver Model

Fig. 2 Inertial reference frame for missile and target

Fig. 3 Typical Missile-Target Trajectories
R_i = Initial range, R_m = Maneuver onset range

Fig. 4 Circular target model filter with different $\Theta's$
$R_i = 6000ft, \quad R_m = 6000ft, \quad \omega = 0.3$

Fig. 5 Circular target model filter with different $V_1's$
$R_i = 6000ft, \quad R_m = 6000ft, \quad \omega = 0.3$

Fig. 6 Circular target model filter with pseudo-measurement
$R_i = 6000ft, \quad R_m = 6000ft, \quad \omega = 0.3$

Fig. 7 Circular target model filter with pseudo-measurement
(A case with different $V_1's$)
$R_i = 6000ft, \quad R_m = 4000ft, \quad \omega = 0.3$

Fig. 8 Circular target model filter with pseudo-measurement
(A case with different $V_1's$)
$R_i = 6000ft, \quad R_m = 4000ft, \quad \omega = 0.3$

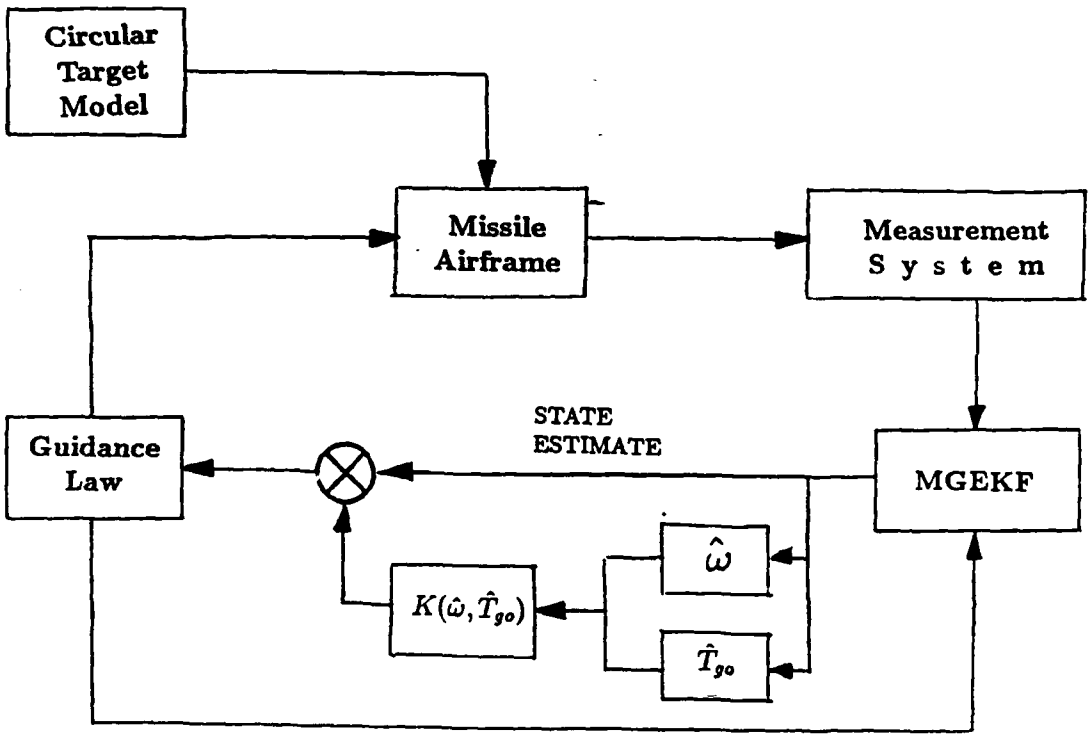

Fig. 1 Diagram of Homing Missile Guidance
Using Circular Target Maneuver Model

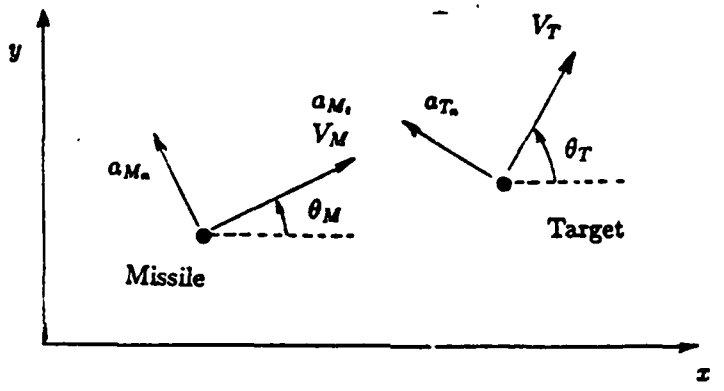

Fig. 2 Inertial reference frame for missile and target

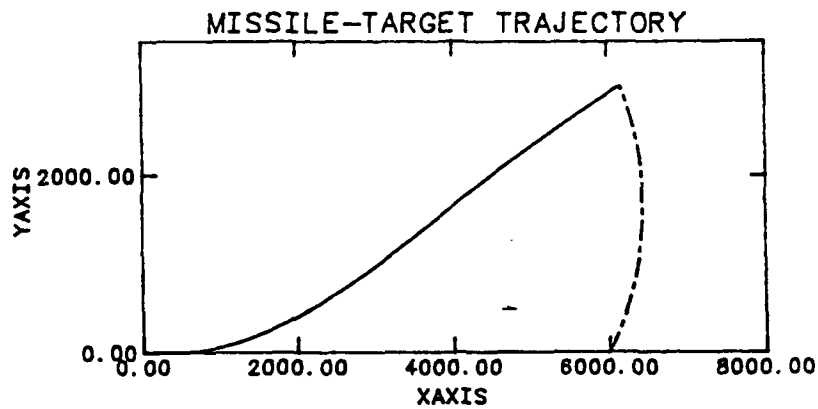

Engagement 1 ($R_i = 6000ft, \quad R_m = 6000ft$)

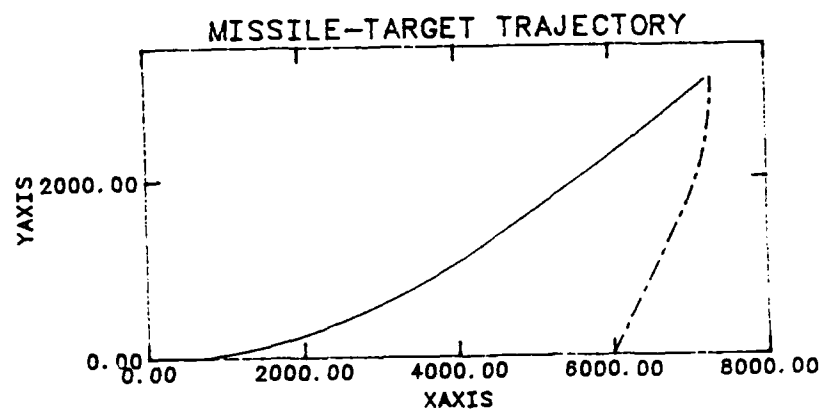

Engagement 2 ($R_i = 6000ft, \quad R_m = 4000ft$)

Fig. 3 Typical Missile-Target Trajectories
R_i = Initial range, R_m = Maneuver onset range

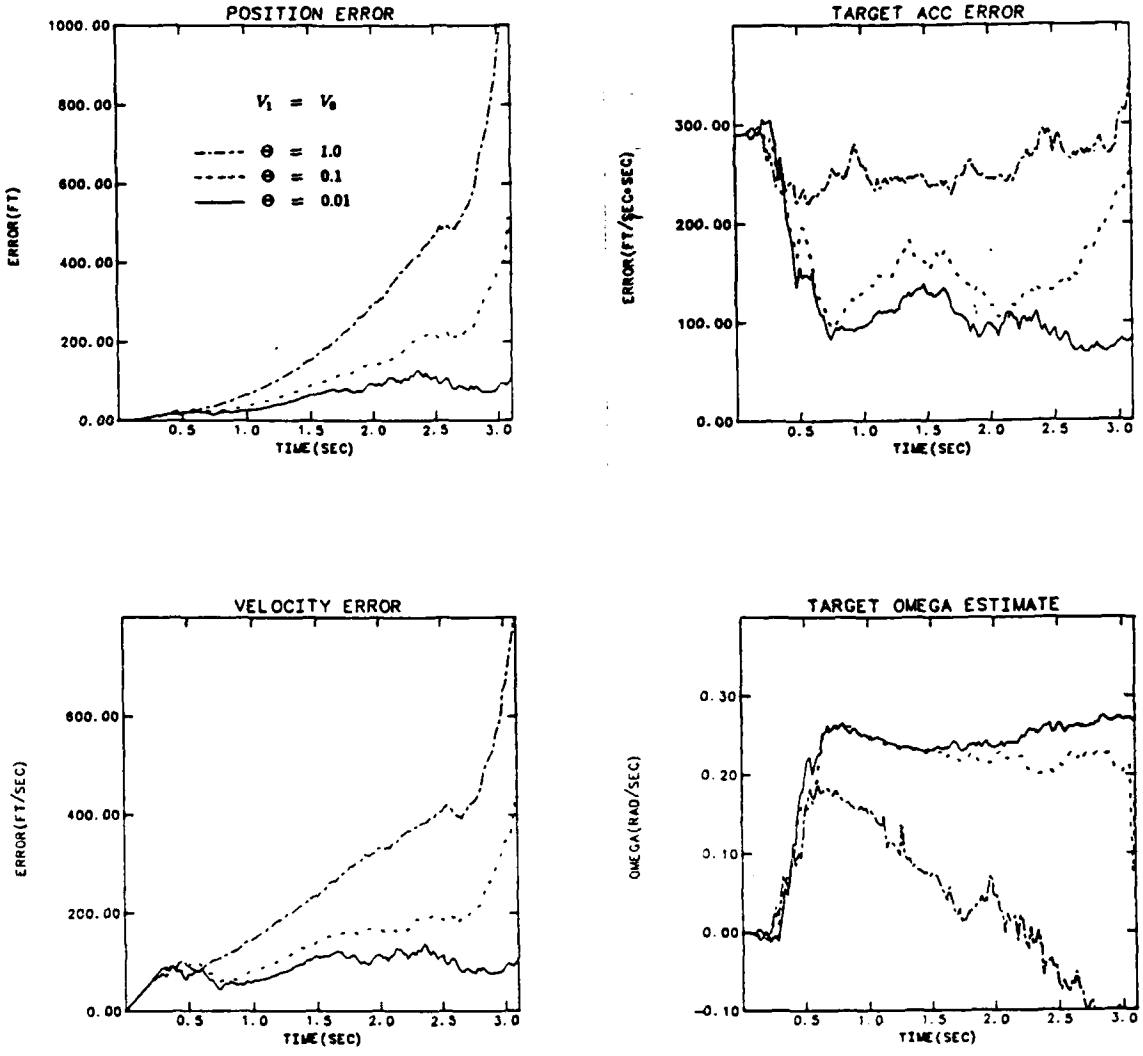

Fig. 4 Circular target model filter with different $\Theta's$
$R_i = 6000ft, \quad R_m = 6000ft, \quad \omega = 0.3$

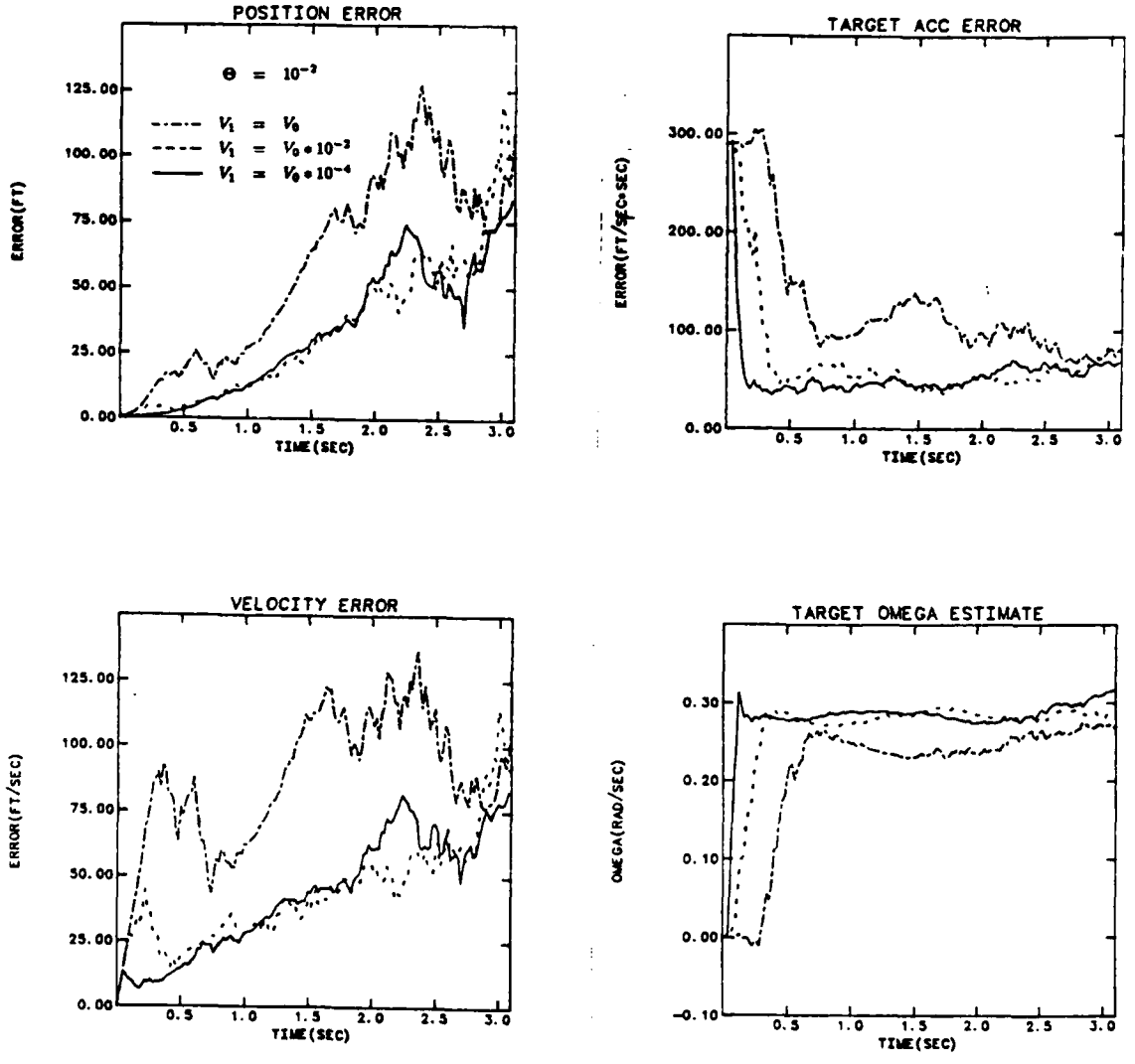

Fig. 5 Circular target model filter with different $V_1's$
$R_i = 6000ft, \quad R_m = 6000ft, \quad \omega = 0.3$

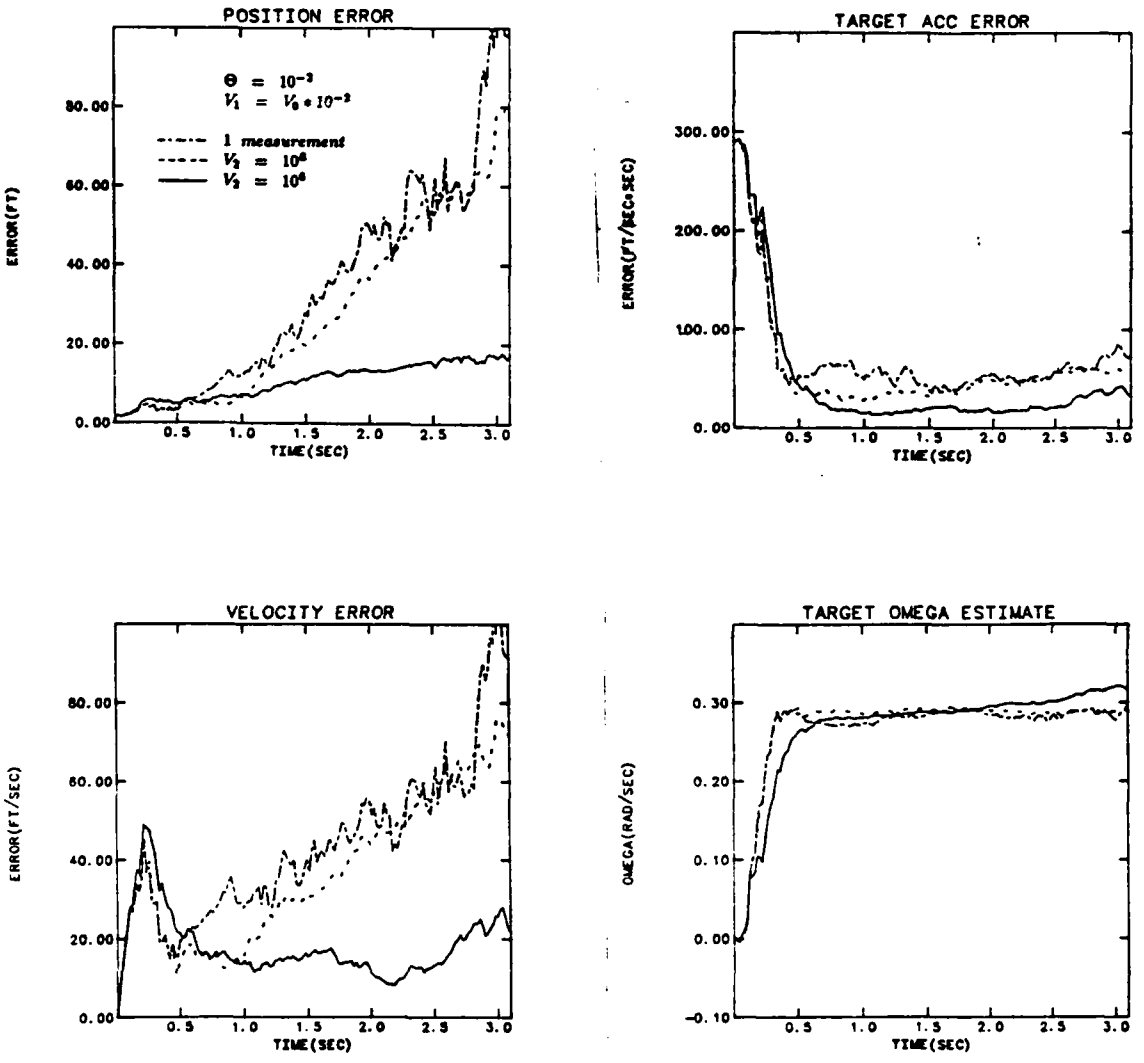

Fig. 6 Circular target model filter with pseudo-measurement
$R_i = 6000ft, \quad R_m = 6000ft, \quad \omega = 0.3$

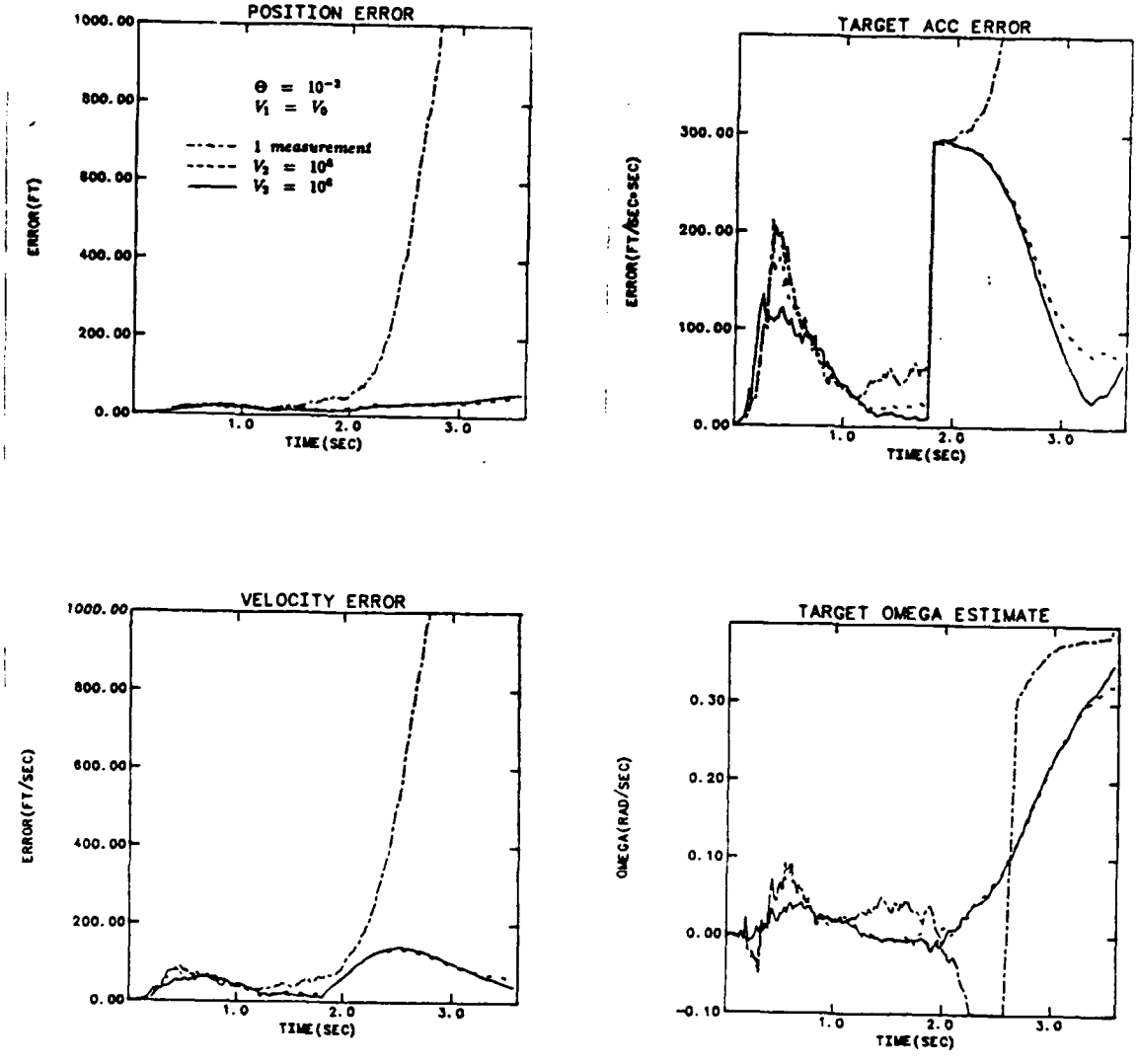

Fig. 7 Circular target model filter with pseudo-measurement (A case with different $V_1's$)
$R_i = 6000ft, \quad R_m = 4000ft, \quad \omega = 0.3$

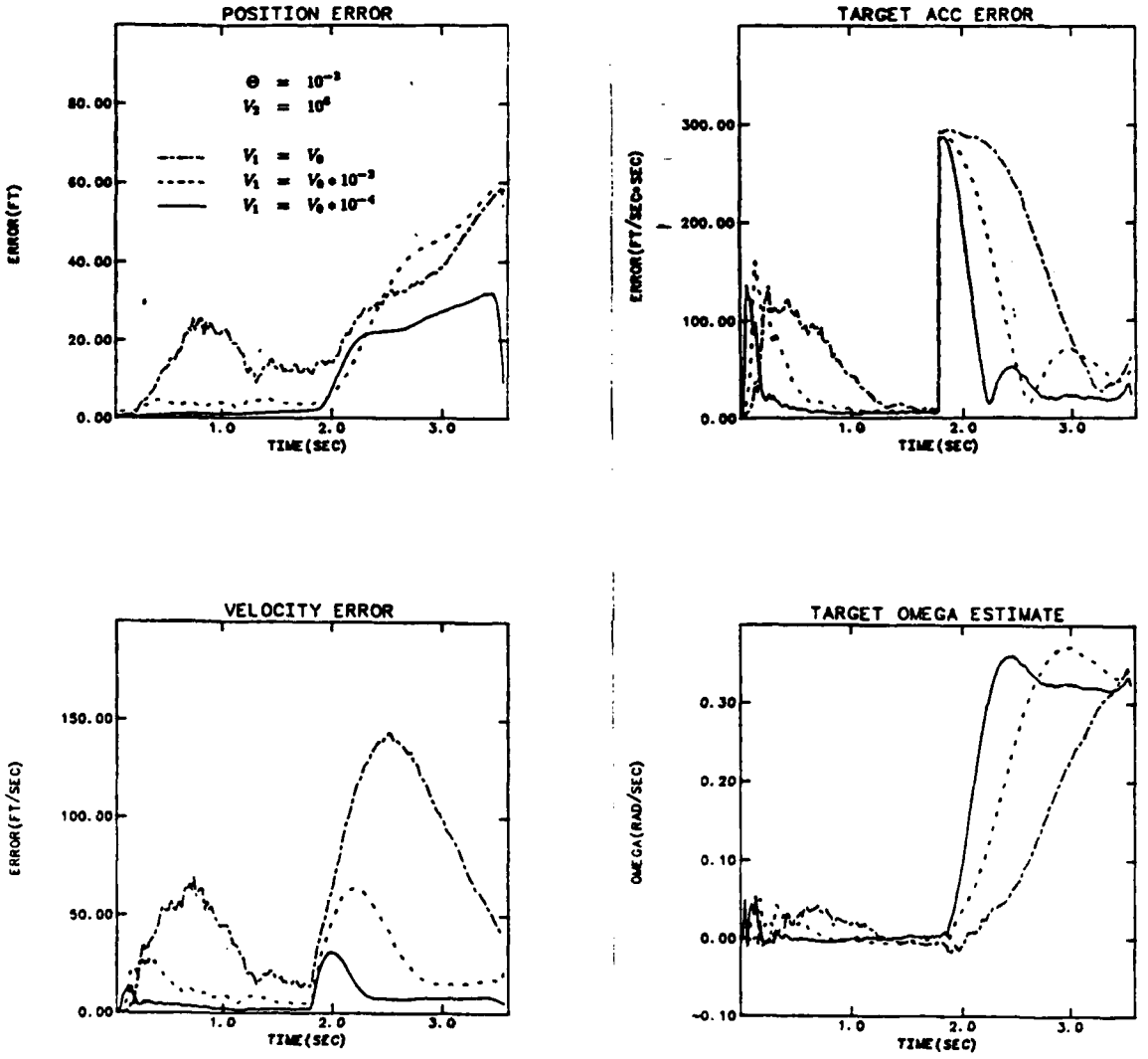

Fig. 8 Circular target model filter with pseudo-measurement
(A case with different $V_1's$)
$R_i = 6000ft, \quad R_m = 4000ft, \quad \omega = 0.3$